Synthesis and direct assembly of linear-dendritic copolymer via CuAAC click polymerization-induced self-assembly (CPISA)

Journal:	*Polymer Chemistry*
Manuscript ID	PY-ART-10-2019-001636.R1
Article Type:	Paper
Date Submitted by the Author:	05-Dec-2019
Complete List of Authors:	Zeng, Min; Tsinghua University, Department of Chemistry Cao, Xiaosong; University of Notre Dame, Department of Chemistry and Biochemistry Xu, Hui; University of Notre Dame, Department of Chemistry and Biochemistry Gan, Weiping; University of Notre Dame, Department of Chemistry & Biochemistry Smith, B.; Notre Dame, Chemistry and Biochemistry, Notre Dame, IN, 46556, USA Gao, Haifeng; Notre Dame, Chemistry and Biochemistry Yuan, Jinying; Tsinghua University, Departmant of Chemistry

SCHOLARONE™
Manuscripts

Synthesis and direct assembly of linear-dendritic copolymer via CuAAC click polymerization-induced self-assembly (CPISA)

Received 00th January 20xx,
Accepted 00th January 20xx

DOI: 10.1039/x0xx00000x

Min Zeng,[a] Xiaosong Cao,[b] Hui Xu,[b] Weiping Gan,[b] Bradley D. Smith,[b] Haifeng Gao*[b] and Jinying Yuan*[a]

A one-pot method was developed for preparation of linear-dendritic copolymer and its assemblies via copper-catalyzed azide-alkyne cycloaddition (CuAAC) click polymerization-induced self-assembly (CPISA). By utilizing a tris-triazoleamine-functionalized poly(ethylene glycol) (PEG) chain as linear macroinitiator and a trifunctional AB_2 with one alkynyl group and two azido groups as monomer, we successfully conducted the CuAAC polymerization in methanol, water, or methanol/water mixture with solids content at 15 wt %. All polymerizations reached high monomer conversion and the rate of polymerization was readily tailored by the fraction of water in the solvent. The polymerization of AB_2 monomer from the PEG macroinitiator produced solvent-insoluble dendritic blocks that assembled under polymerization conditions to form spherical micelles and large compound micelles, characterized by dynamic light scattering and transmission electron microscopy. This strategy broadens the topological architecture of copolymers synthesized by PISA process and puts forward a new methodology for direct preparation of nanostructures based on linear-dendritic polymers.

Introduction

Self-assembly of block copolymers provides a powerful method to prepare polymeric nanomaterials with varied morphologies and functionalities.[1-6] Despite advances, traditional self-assembly strategies are often conducted at low polymer concentration (< 1 wt %) and require multiple steps, limiting large-scale fabrication of materials and in-depth exploration of their applications.[7, 8] Recently, polymerization-induced self-assembly (PISA) emerged as an alternative one-pot technique for in situ preparation of polymeric nanoparticles at high solid concentrations (typically > 10 wt %).[9-22] PISA is usually conducted in dispersion or emulsion conditions, where polymerization induces system heterogeneity and polymer assembly. In other words, soluble polymer in a proper solvent becomes insoluble after chain extension by polymerization of a second monomer, resulting in the assembly of amphiphilic copolymers into nanoparticles.

To date, PISA has been predominantly performed using various types of controlled/living radical polymerization techniques, most notably, reversible addition-fragmentation chain transfer (RAFT) polymerization.[22-32] Due to the requirements of PISA process and the mechanism of RAFT polymerization, most reported PISA-made nanoparticles are composed of linear block copolymers.[33-37] As polymer architecture is a well-known parameter to the morphology of block copolymer assemblies and has profound influence on their functions,[38] it is initially surprising to realize that very few studies have been published on approaching nonlinear polymer structures using PISA technique. For example, Zhang and coworkers designed star block copolymer assemblies using 3- and 4-arm star poly(4-vinylpyridine) macromolecular chain transfer agents (macro-CTA) via RAFT dispersion polymerization processes.[39] By increasing the number of arms, several interesting morphologies of the star block copolymer assemblies, including small-sized vesicles, lacunal nanospheres, and porous nanospheres, could be prepared. Similarly, Sumerlin and An et al. reported the synthesis of star block copolymer assemblies via RAFT dispersion polymerization by using a two-CTA modified poly(ethylene glycol) as macro-CTA.[29] Besides these star block copolymer structures, it is within our best knowledge that there has been no report on synthesis and assembly of branched amphiphilic block copolymers using PISA processes.

Linear-dendritic copolymers are emerging as an attractive category of block copolymer in both academia and industry as the polymer by combining the linear chains and dendritic structures exhibit excellent properties, such as good encapsulation, multiple chain-end functionalities and unique self-assembly properties.[40-44] Self-assembly of amphiphilic linear-dendritic copolymers has become an active area in self-assembling materials. However, traditional self-assembly techniques for linear-dendritic copolymers were limited to low solids content and require multiple steps, which largely preclude their scale-up. As a result, development of a new strategy for the self-assembly of linear-dendritic copolymers with high solids content is still needed.

Hyperbranched (or highly branched) polymers, as an important type of dendritic polymers, have attracted great attention owing to their fascinating features including one-pot

---

[a] *Key Lab of Organic Optoelectronics and Molecular Engineering of Ministry of Education, Department of Chemistry, Tsinghua University, 100084, Beijing, China. E-mail: yuanjy@mail.tsinghua.edu.cn*

[b] *Department of Chemistry and Biochemistry, University of Notre Dame, Notre Dame, Indiana 46556, United States. E-mail: hgao@nd.edu*

Electronic Supplementary Information (ESI) available: [details of any supplementary information available should be included here]. See DOI: 10.1039/x0xx00000x syntheses, high degree of functionalization, and arborescent structures.[45-59] To synthesize hyperbranched polymers with controlled structures, Gao group has recently reported a living chain-growth polymerization of trifunctional AB_2 monomer via copper-catalyzed azide-alkyne cycloaddition (CuAAC) reaction.[60-64] This method, exhibiting both high monomer conversion and well-defined chain-growth polymerization, could potentially be applied in biphasic dispersion systems to achieve assembled structures of hyperbranched polymers. In this contribution, we for the first time developed a PISA method for CuAAC polymerization of AB_2 monomers to prepare linear-dendritic copolymers and their assemblies via CuAAC-based PISA (CPISA, Scheme 1). The AB_2-Bn monomer with benzyl pendant and a tris-triazoleamine-functionalized poly(ethylene glycol) (PEG_{112}-B_2) macroinitiator were synthesized. Both dispersion and emulsion CuAAC polymerizations of AB_2-Bn were performed to prepare linear-dendritic copolymer assemblies in one-pot.

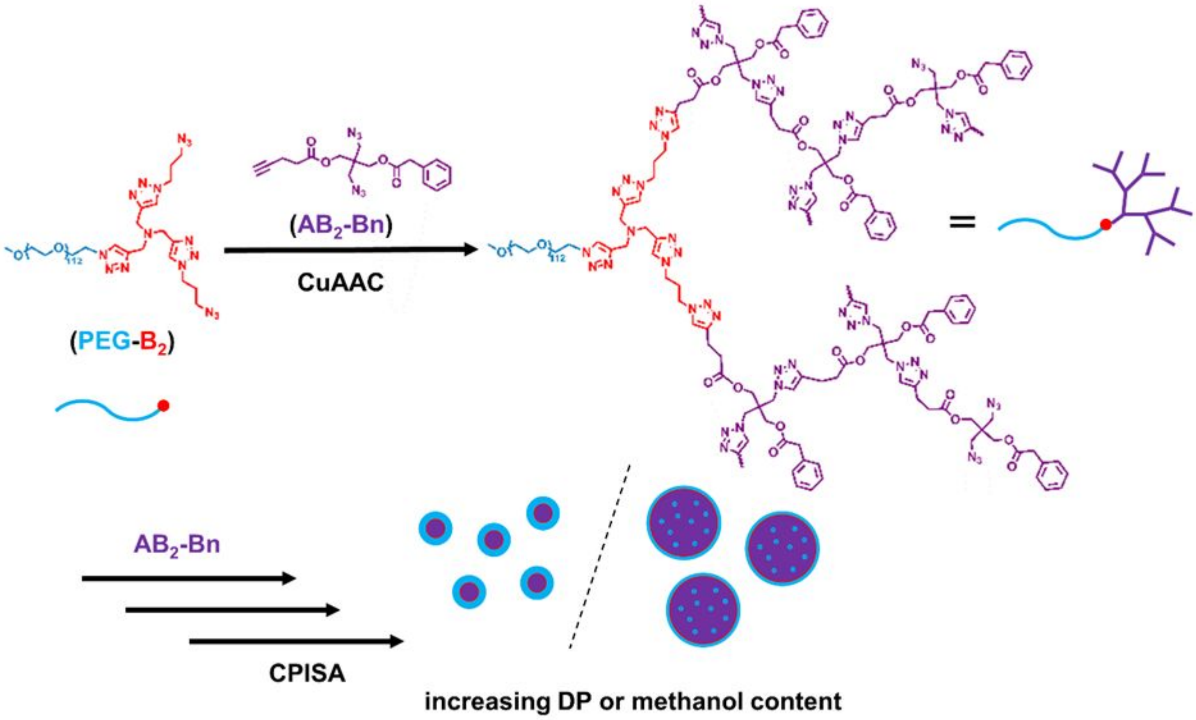

Scheme 1 The synthetic routes to linear-dendritic copolymer assemblies via CuAAC click polymerization-induced self-assembly (CPISA).

Results and discussion

Synthesis of PEG_{112}-B_2 macroinitiator

To prepare the macroinitiator stabilizer block, a tris-triazoleamine-functionalized poly(ethylene glycol) (PEG_{112}-B_2) that contained two terminal azido groups (Scheme 2) was designed and synthesized. Our previous results confirm that the central tris-triazoleamine motif shows strong complexation with Cu(I) catalyst and predominatly confines the Cu catalyst to the PEG macroinitiator even before the polymerization of AB_2 monomer.[61, 65] The detailed synthesis and molecular characterization were provided in the supporting information. ^1H NMR spectroscopy and size exclusion chromatography (SEC) were used to characterize the chemical structure and molecular weight of PEG_{112}-B_2 macroinitiator, respectively (Fig. 1). The degree of end-group functionalization of PEG_{112} can be estimated by the area ratio of the signal at $\delta = 2.17$ ppm (b in Fig. 1A) and the signal at $\delta = 4.55$ ppm (f in Fig. 1A), and it is suggested that the degree of end-group functionalization is

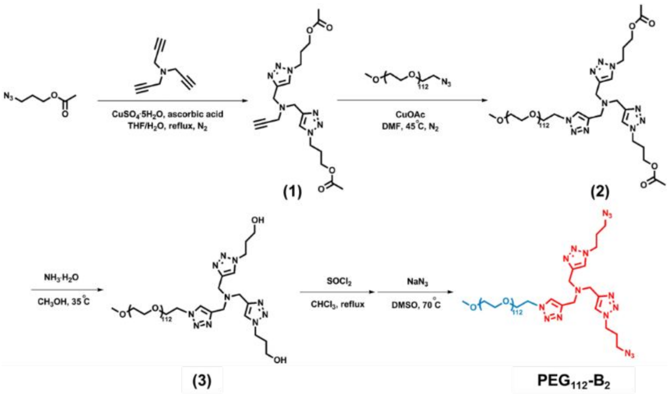

Scheme 2 The synthetic routes to PEG_{112}-B_2 macroinitiator.

This journal is © The Royal Society of Chemistry 20xx

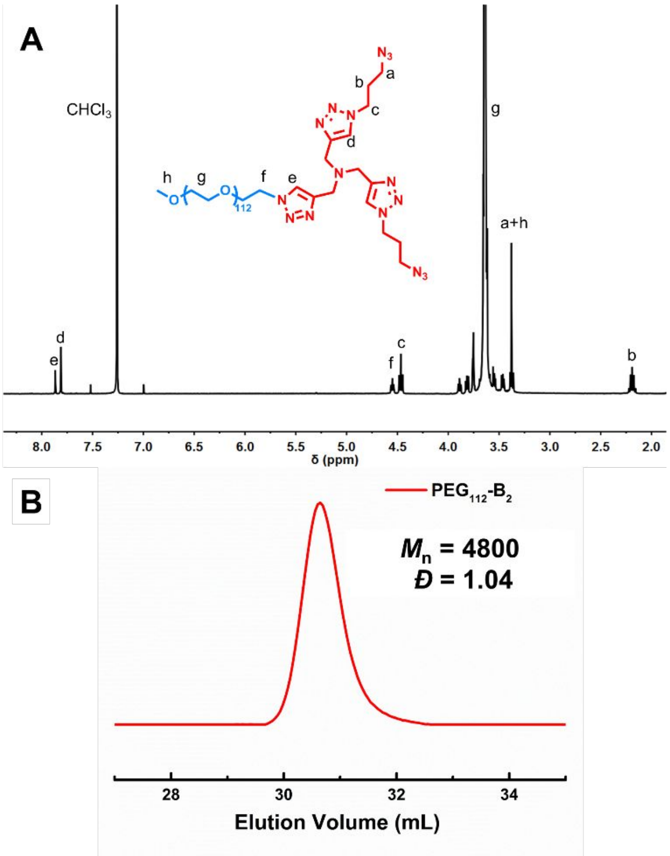

Fig. 1 A) ^{1}H NMR spectrum of PEG$_{112}$-B$_2$ with CDCl$_3$ as solvent at 25 °C; B) SEC trace recorded for PEG$_{112}$-B$_2$.

more than 97%. In SEC with DMF as mobile phase, the PEG$_{112}$-B$_2$ showed an apparent number-average molecular weight $M_{n,RI}$ = 4,800 with a low polydispersity $Đ$ = 1.04, based on linear poly(methyl methacrylate) PMMA standards with refractive index (RI) detector.

Synthesis and direct assembly of PEG$_{112}$-p(AB$_2$-Bn)$_x$ via CPISA

To demonstrate the synthesis and assembly of linear-dendritic polymers under CPISA condition, an AB$_2$-Bn monomer (Scheme 1, S1 and Fig. S1) carrying a benzyl (Bn) pendant group was selected for CuAAC polymerization using the PEG$_{112}$-B$_2$ as macroinitiator, in which proper solvents or their mixture was critical to ensure the second hyperbranched block was not soluble and could self-assemble into nanostructures, such as core-shell structures. As the first attempt, a CuAAC polymerization of the AB$_2$-Bn monomer was carried out in the mixture of methanol/water (90/10, by wt) at 45 °C using a feed ratio of [AB$_2$-Bn]$_0$/[PEG$_{112}$-B$_2$]$_0$ = 80/1. The polymerization was conducted at 15 wt % solids content, which was much higher than that in the co-solvent method for assembly of preformed amphiphilic block copolymer (usually < 1 wt %).[9] As the polymerization started, kinetic studies were performed by taking a series of aliquot samples at different times. As shown in Fig. 2A, the conversions of AB$_2$-Bn monomer increased with polymerization time and reached 98% within 24 h, determined by ^{1}H NMR spectroscopy. SEC characterization of purified polymers showed increased apparent molecular weight of the polymer product as a function of AB$_2$-Bn monomer conversion (Fig. 2B). This result confirmed the polymerization of monomers and the production of linear-dendritic copolymers although a shoulder peak at low volume direction and an oligomer peak existed in the SEC curves, probably due to the undesired monomer-monomer reaction in parallel to the desired monomer polymerization from the macroinitiator (Fig. S2). Meanwhile, the progress of polymerization changed the reaction system from transparent solution to translucent dispersion after 0.5 h, indicating the generation of assembled nanostructures whose hydrodynamic diameters increased and finally reached 215 nm after 24 h (Fig. 2C) when the polymerization was completed.

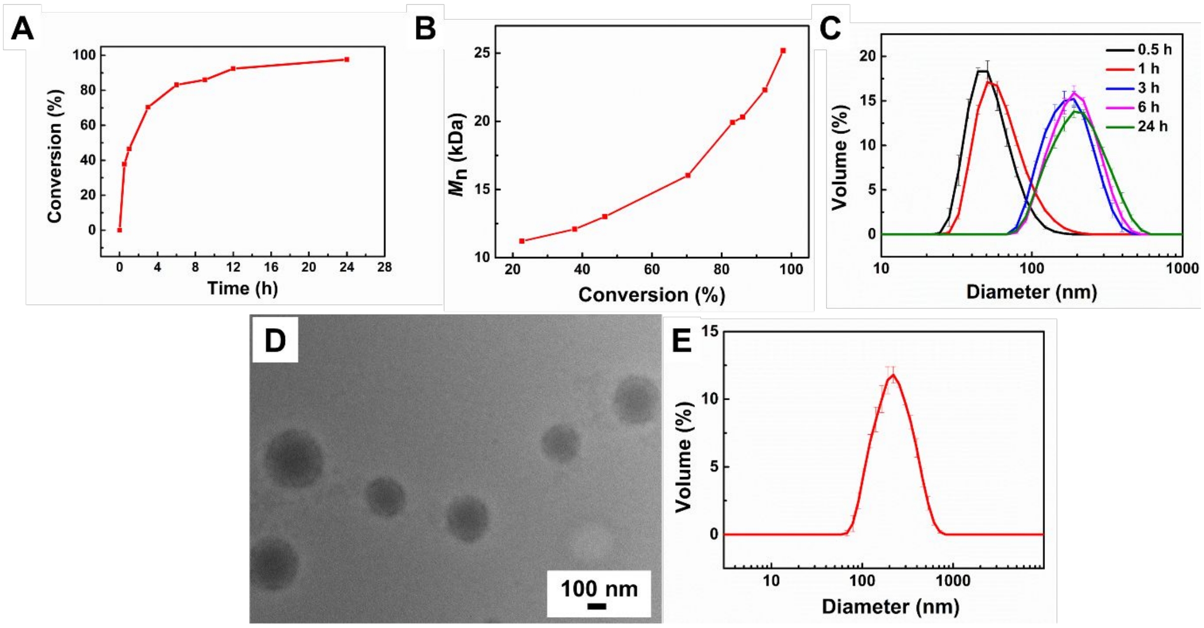

Fig. 2 A) Conversion, B) evolution of M_n with the monomer conversion and C) DLS characterization of the PEG$_{112}$-p(AB$_2$-Bn)$_{80}$ assemblies as a function of time prepared via dispersion CuAAC polymerization in methanol/water (90/10, by wt) at 45 °C; D) TEM image and E) DLS characterization of the PEG$_{112}$-p(AB$_2$-Bn)$_{80}$ assemblies.

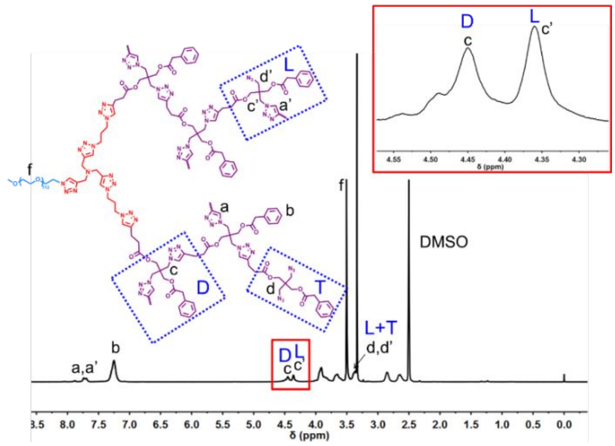

Fig. 3 ^{1}H NMR spectrum of PEG_{112}-p(AB_2-Bn)$_{80}$ with DMSO-d6 as solvent at 25 °C.

After polymerization, a portion of the polymer product was purified to characterize the polymer structures and molecular weights by ^{1}H NMR and SEC, while another portion of the samples were prepared for characterization of polymer assemblies using transmission electron microscopy (TEM) and dynamic light scattering (DLS). The ^{1}H NMR spectrum of purified polymer PEG_{112}-p(AB_2-Bn)$_{80}$ (Fig. 3) indicates resolved peaks from both PEG_{112} and p(AB_2-Bn)$_{80}$ blocks. By comparing the methylene proton peak (f in Fig. 3) from the PEG_{112} block and the phenyl proton peak (b in Fig. 3) from the p(AB_2-Bn)$_{80}$ block, the integral area ratio of peak b and f was consistent with the feed ratio of $[AB_2\text{-}B_n]_0/[PEG_{112}\text{-}B_2]_0$ and high monomer conversion. This result further confirmed the successful synthesis of linear-dendritic copolymer PEG_{112}-p(AB_2-Bn)$_{80}$ and the high monomer conversion of CPISA strategy. The degree of branching (DB) of purified polymer PEG_{112}-p(AB_2-Bn)$_{80}$ was determined by ^{1}H NMR spectroscopy by following published method.[64, 66] The calculated result based on equation DB = 2D/(2D + L) was about DB = 0.53, in which D and L represent the mole fraction of dendritic unit and linear unit in the hyperbranched polymer quantified by integrating the peaks of c and c′. It is worth noting this DB value was lower than that of hyperbranched polymers synthesized in solution CuAAC polymerization (e.g., DB > 0.80)[64] primarily because the partition of Cu(I) catalysts between the organic polymer phase and the continuous methanol/water phase. Due to the charged nature of Cu(I) catalyst, its escape from the polymerizing particle into the methanol/water phase decreased the effective concentration and residing time of Cu catalyst on the L unit in the polymer, resulting in a slower reaction of the dangling azido group to convert L unit to D unit and a lower DB value of the polymer.

Table 1. Summary of the linear-dendritic copolymers PEG_{112}-p(AB_2-Bn)$_x$ and their assemblies.

Entry	Solvent CH_3OH/H_2O by wt	Feed ($[PEG_{112}\text{-}B_2]_0$/ $[AB_2\text{-}Bn]_0$)	Conv.^{a}(%)	$M_{n,\ MALLS}$^{b}	DB^c	$M_{n,\ RI}$^{d}	$Đ$^{d}	DLS	
								D_h^{e}(nm)	PdI^e
1	100/0	1/20	96	18400	0.47	13000	1.19	23	0.092
2	100/0	1/40	98	41600	0.52	22100	1.07	84	0.260
3	100/0	1/80	96	73700	0.53	31000	1.19	1031	0.290
4	100/0	1/120	97	95400	0.52	36300	1.34	1368	0.460
5	95/5	1/80	99	82500	0.52	25200	1.63	1093	0.309
6	90/10	1/20	99	29700	0.52	16200	1.28	34	0.083
7	90/10	1/40	99	34500	0.53	19700	1.31	91	0.302
8	90/10	1/80	98	70900	0.53	24500	1.45	237	0.136
9	90/10	1/120	98	113200	0.52	40600	1.40	320	0.099
10	0/100	1/80	93	67900	0.51	33400	1.68	34	0.286

[a] Monomer AB_2-Bn conversion determined by ^{1}H NMR spectroscopy. [b] Absolute number-average molecular weight ($M_{n,MALLS}$) determined by DMF SEC with a MALLS detector. [c] Degree of branching (DB) determined by ^{1}H NMR spectroscopy. [d] Apparent number-average molecular weight ($M_{n,RI}$) and molecular weight distribution ($Đ = M_w/M_n$) determined by DMF SEC with a RI detector based on linear PMMA standards. [e] Hydrodynamic diameter (D_h) and polydispersity index (PdI) determined by DLS analysis of the assembly samples in corresponding reaction solvent after dialysis.

Meanwhile, characterization of the polymers by SEC coupled with multi-angle laser light scattering (MALLS) detector and RI detector determined the absolute number-average molecular weights $M_{\mathrm{n,\ MALLS}}$ = 70,900 and the $M_{\mathrm{n,RI}}$ = 24,500 (Table 1, entry 8). The higher value of $M_{\mathrm{n,\ MALLS}}$ than $M_{\mathrm{n,RI}}$ indicates a compact molecular structure of the linear-dendritic copolymer.

In addition to determining the molecular characteristics, the assembled nanostructures in dispersion were characterized by both TEM and DLS. Fig. 2D suggests spherical micelles were obtained from the PEG_{112}-p(AB_2-Bn)$_{80}$ assemblies, and DLS result in Fig. 2E shows the hydrodynamic diameter (D_h) of these assemblies was D_h = 237 nm with a narrow size distribution of 0.136. These results suggested the successful CPISA process to form well-defined micellar structures by using mixed solvent of methanol/water via dispersion CuAAC polymerization of AB_2-Bn monomer.

Based on the initial success as discussed above, several other linear-dendritic copolymer assemblies with varied DPs of the hyperbranched segment, i.e. , PEG_{112}-p(AB_2-Bn)$_x$ with x = 20, 40, 120, were produced using similar procedures, in order to explore morphological evolution of the assemblies as a function of molecular weights of dendritic segment. Each polymerization was carried out in methanol/water (90/10, by wt) with solids content at 15 wt %. In all these polymerizations, high monomer conversion (≥ 98 %) were achieved before the polymerizations were stopped. It was found that the hydrodynamic diameter of these linear-dendritic copolymer assemblies increased from D_h = 34 to 320 nm as the feed ratio of AB_2-Bn monomer to PEG macroinitiator increasing from x = 20 to 120 (Fig. 4D). TEM results indicated spherical micelles for all three PEG_{112}-p(AB_2-Bn)$_x$ (x = 20, 40, 120) linear-dendritic copolymer assemblies (Fig. 4A-4C). As the length of PEG stabilizer block has great influence on the final morphologies, the long PEG_{112} block led to effective steric stabilization of the hydrophobic dendritic block and prevented evolution in copolymer morphology,[67-69] so that the variation of x between 20 and 120 resulted in the spherical morphology of the assembled nanostructures.

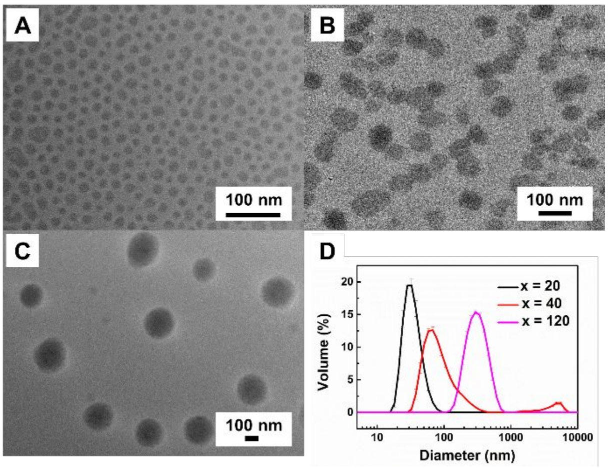

Fig. 4 TEM images of A) PEG_{112}-p(AB_2-Bn)$_{20}$, B) PEG_{112}-p(AB_2-Bn)$_{40}$ C) PEG_{112}-p(AB_2-Bn)$_{120}$ assemblies, and D) DLS characterizations of PEG_{112}-p(AB_2-Bn)$_x$ (x = 20, 40, 120) assemblies prepared via dispersion CuAAC polymerization in methanol/water (90/10, by wt) at 45 °C.

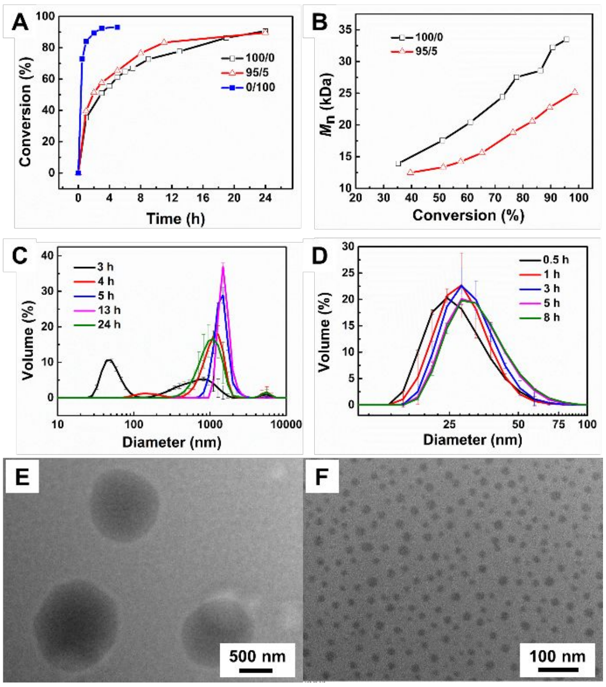

Fig. 5 A) Evolution of monomer conversions with time in the preparation of PEG_{112}-p(AB_2-Bn)$_{80}$ by CuAAC polymerization in methanol (100/0), methanol/water (95/5, by wt), and water (0/100); B) evolution of $M_{\mathrm{n,RI}}$ with monomer conversion in preparation of PEG_{112}-p(AB_2-Bn)$_{80}$ by CuAAC polymerization in methanol (100/0) and methanol/water (95/5, by wt); DLS characterization of the PEG_{112}-p(AB_2-Bn)$_{80}$ assemblies as a function of time prepared via CPISA in C) methanol (100/0) and D) water (0/100); TEM images of the final PEG_{112}-p(AB_2-Bn)$_{80}$ assemblies prepared via CPISA in E) methanol (100/0) and F) water (0/100).

Besides altering the size of dendritic block, we further evaluated the influence of solvents on the structures of linear-dendritic copolymers and their assembly morphology, since solvent is an important factor in CPISA process. For comparison, several CuAAC polymerizations of AB_2-Bn with a target composition of PEG_{112}-(AB_2-Bn)$_{80}$ were performed in methanol (100/0), methanol/water (95/5, by wt), and water (0/100), respectively (Table 1). All polymerizations carried out at 45 °C reached high monomer conversions although the polymerization rate increased with the content of water in the solvent. For instance, the CPISA in pure water observed the fastest polymerization and reached 93% monomer conversion in 5 h (Fig. 5A). As the AB_2-Bn monomer is insoluble in water, the CPISA system formed emulsion before polymerization. The PEG macroinitiator assisted the emulsification of monomers into discrete micelles and droplets, which facilitated faster polymerization due to neat monomer concentration inside and compartmentalization effect.[70] Regarding the molecular weight evolution, all polymerizations showed increased polymer molecular weights i.e., $M_{n,RI}$, with conversion as shown in Fig. 5B. Meanwhile, the molecular weight of polymer from CPISA in pure methanol (100/0) was larger than that from the mixed solvent methanol/water (95/5, by wt), probably due the different extent of monomer-monomer reactions in these systems. As competing with the monomer-polymer reaction, the monomer-monomer reaction formed oligomers and decreased the overall molecular weight of the linear-dendritic copolymer.

Interestingly, DLS characterizations of the PEG_{112}-p(AB_2-Bn)$_{80}$ assemblies prepared via CPISA in methanol and water were significantly different. For the polymerization in methanol, the D_h of the assemblies increased from D_h = 52 to 1416 nm, and eventually stabilized at 1031 nm (Fig. 5C). The degree of solvation of methanol and AB_2-Bn monomer to the assemblies decreased as the polymerization proceeded, which resulted in the size of assemblies slight decreased after polymerization for 24 h.[70, 71] TEM image in Fig. 5E reveals their morphology to be large compound micelles as the dimension of assemblies was much larger than the extended contour length of linear dendritic polymer. This result was in agreement with the observed large D_h size of the PEG_{112}-(AB_2-Bn)$_{80}$ assemblies in methanol, indicating entangled PEG chain embedded inside the compound micelles.[72] Similarly, large compound micelles were also obtained in PEG_{112}-p(AB_2-Bn)$_{80}$ assemblies prepared in methanol/water (95/5, by wt) (Fig. S3). For the CPISA in water, the hydrodynamic size of assemblies varied in a narrow range from D_h 28 to 33 nm (Fig. 5D) as the CuAAC polymerization of water-insoluble AB_2-Bn monomer in water was an emulsion instead of a dispersion. TEM confirms that spherical micelles were obtained for the PEG_{112}-(AB_2-Bn)$_{80}$ assemblies synthesized in water (Fig. 5F).

Since the CPISA in pure methanol reassembled a true dispersion polymerization system and produced large compound micelles as product, further studies were carried out to prepare a series of PEG_{112}-p(AB_2-Bn)$_x$ (x = 20, 40, 80, 120) linear- dendritic copolymer assemblies in methanol (Table 1). Along with PEG_{112}-p(AB_2-Bn)$_{80}$ assemblies, the D_h of these four assemblies increased from 23 to 1368 nm and the morphology transformed from spherical micelles to large compound micelles with the increase of the DP of the solvophobic blocks (Fig. 6A-6D). When considering both series of PEG_{112}-p(AB_2-Bn)$_x$ assemblies with varied x values and different solvents as methanol/water (90/10, by wt) or pure methanol, it was confirmed that both the molecular size of dendritic block and polymerization solvent were vital to the morphologies of assembled nanostructures in these CPISA systems.

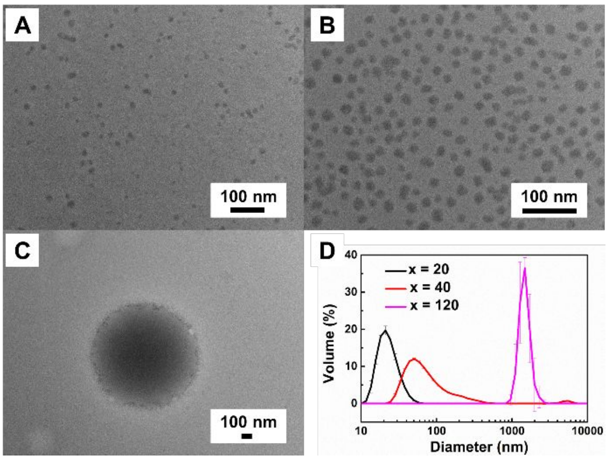

Fig. 6 TEM images of A) PEG_{112}-p(AB_2-Bn)$_{20}$, B) PEG_{112}-p(AB_2-Bn)$_{40}$, C) PEG_{112}-p(AB_2-Bn)$_{120}$ assemblies, and D) DLS characterizations of PEG_{112}-p(AB_2-Bn)$_x$ (x = 20, 40, 120) assemblies prepared via CPISA in methanol.

Conclusions

In summary, we successfully developed a method to fabricate linear-dendritic copolymer and its assemblies via CuAAC polymerization using the PISA formula. This strategy, termed as CPISA, was performed in various solvents, including methanol, methanol/water mixture and water, to target different DPs of the dendritic block in high conversions. Both experimental variables, the solvent and the DP, exhibited significant effect on the polymerization kinetics and the morphology of the assemblies. Higher water content not only increased the polymerization rate, but also produced micelle-like linear-dendritic polymer assemblies. Meanwhile, pure methanol as solvent and higher target DP produced large compound micelles as the CPISA in water started as emulsion while the CPISA in methanol stared as solution before the polymerization-induced assembly progressed with monomer conversion. These results demonstrate for the first time the preparation of linear-dendritic copolymer assemblies via CPISA process and provide a useful approach to fabricate nanostructured assemblies based on dendritic polymers for potential applications.

Conflicts of interest

There are no conflicts to declare.

Acknowledgements

The National Natural Science Foundation of China (Project Nos. 51573086 and 21871162) is acknowledged for financial support. M.Z. thanks the Tsinghua Scholarship for Overseas Graduates Studies. H.G. thanks the National Science Foundation (CHE-1554519) for financial support. M.Z., B.D.S. and H.G. thank Asia Research Collaboration Grant, Notre Dame International for partial support of this research.

References

1 Y. Mai and A. Eisenberg, *Chem. Soc. Rev.*, 2012, **41**, 5969-5985.
2 U. Tritschler, S. Pearce, J. Gwyther, G. R. Whittell and I. Manners, *Macromolecules*, 2017, **50**, 3439-3463.
3 A. Blanazs, S. P. Armes and A. J. Ryan, *Macromol. Rapid Commun.*, 2009, **30**, 267-277.
4 A. Rösler, G. W. M. Vandermeulen and H.-A. Klok, *Adv. Drug Deliv. Rev.*, 2012, **64**, 270-279.
5 R. C. Hayward and D. J. Pochan, *Macromolecules*, 2010, **43**, 3577-3584.
6 J. K. Kim, S. Y. Yang, Y. Lee and Y. Kim, *Prog. Polym. Sci.*, 2010, **35**, 1325-1349.
7 N. S. Cameron, M. K. Corbierre and A. Eisenberg, *Can. J. Chem.*, 1999, **77**, 1311-1326.
8 Y. Wang, M. Huo, M. Zeng, L. Liu, Q.-Q. Ye, X. Chen, D. Li, L. Peng and J.-Y. Yuan, *Chin. J. Polym. Sci.*, 2018, **36**, 1321-1327.
9 S. L. Canning, G. N. Smith and S. P. Armes, *Macromolecules*, 2016, **49**, 1985-2001.
10 B. Charleux, G. Delaittre, J. Rieger and F. D'Agosto, *Macromolecules*, 2012, **45**, 6753-6765.
11 W.-M. Wan, X.-L. Sun and C.-Y. Pan, *Macromolecules*, 2009, **42**, 4950-4952.
12 S.-l. Chen, P.-f. Shi and W.-q. Zhang, *Chin. J. Polym. Sci.*, 2017, **35**, 455-479.
13 M. Huo, G. Song, J. Zhang, Y. Wei and J. Yuan, *ACS Macro Lett.*, 2018, **7**, 956-961.
14 X.-L. Sun, D.-M. Liu, P. Wang, J.-L. Tan, K.-K. Li, L. Deng and W.-M. Wan, *Chem. Commun.*, 2017, **53**, 5005-5008.
15 S. Guan, Z. Deng, T. Huang, W. Wen, Y. Zhao and A. Chen, *ACS Macro Lett.*, 2019, **8**, 460-465.
16 J. C. Foster, S. Varlas, B. Couturaud, J. R. Jones, R. Keogh, R. T. Mathers and R. K. O'Reilly, *Angew. Chem. Int. Ed.*, 2018, **57**, 15733-15737.
17 J. C. Foster, S. Varlas, L. D. Blackman, L. A. Arkinstall and R. K. O'Reilly, *Angew. Chem. Int. Ed.*, 2018, **57**, 10672-10676.
18 X. Wang and Z. An, *Macromol. Rapid Commun.*, 2019, **40**, 1800325.
19 J. Tan, X. Dai, Y. Zhang, L. Yu, H. Sun and L. Zhang, *ACS Macro Lett.*, 2019, **8**, 205-212.
20 X.-F. Xu, C.-Y. Pan, W.-J. Zhang and C.-Y. Hong, *Macromolecules*, 2019, **52**, 1965-1975.
21 S. Varlas, L. D. Blackman, H. E. Findlay, E. Reading, P. J. Booth, M. I. Gibson and R. K. O'Reilly, *Macromolecules*, 2018, **51**, 6190-6201.
22 C. A. Figg, R. N. Carmean, K. C. Bentz, S. Mukherjee, D. A. Savin and B. S. Sumerlin, *Macromolecules*, 2017, **50**, 935-943.
23 J. Rieger, *Macromol. Rapid Commun.*, 2015, **36**, 1458-1471.
24 X. Chen, L. Liu, M. Huo, M. Zeng, L. Peng, A. Feng, X. Wang and J. Yuan, *Angew. Chem. Int. Ed.*, 2017, **56**, 16541-16545.
25 M. Zeng, M. Huo, Y. Feng and J. Yuan, *Macromol. Rapid Commun.*, 2018, **39**, 1800291.
26 J.-T. Sun, C.-Y. Hong and C.-Y. Pan, *Polym. Chem.*, 2013, **4**, 873-881.
27 Q. Ye, M. Huo, M. Zeng, L. Liu, L. Peng, X. Wang and J. Yuan, *Macromolecules*, 2018, **51**, 3308-3314.
28 M. A. Touve, C. A. Figg, D. B. Wright, C. Park, J. Cantlon, B. S. Sumerlin and N. C. Gianneschi, *ACS Cent. Sci.*, 2018, **4**, 543-547.
29 X. Wang, C. A. Figg, X. Lv, Y. Yang, B. S. Sumerlin and Z. An, *ACS Macro Lett.*, 2017, **6**, 337-342.
30 S. Qu, R. Liu, W. Duan and W. Zhang, *Macromolecules*, 2019, **52**, 5168-5176.
31 M. Chen, J.-W. Li, W.-J. Zhang, C.-Y. Hong and C.-Y. Pan, *Macromolecules*, 2019, **52**, 1140-1149.
32 C. A. Figg, A. Simula, K. A. Gebre, B. S. Tucker, D. M. Haddleton and B. S. Sumerlin, *Chem. Sci.*, 2015, **6**, 1230-1236.
33 W. Cai, W. Wan, C. Hong, C. Huang and C. Pan, *Soft Matter*, 2010, **6**, 5554-5561.
34 M. Huo, Y. Zhang, M. Zeng, L. Liu, Y. Wei and J. Yuan, *Macromolecules*, 2017, **50**, 8192-8201.
35 J. Tan, Q. Xu, Y. Zhang, C. Huang, X. Li, J. He and L. Zhang, *Macromolecules*, 2018, **51**, 7396-7406.
36 A. A. Cockram, T. J. Neal, M. J. Derry, O. O. Mykhaylyk, N. S. J. Williams, M. W. Murray, S. N. Emmett and S. P. Armes, *Macromolecules*, 2017, **50**, 796-802.
37 Q.-q. Ye, M.-x. Zheng, X. Chen, D. Li, W.-g. Tian, J. Zhang and J.-y. Yuan, *Acta Polym. Sin.*, 2019, **50**, 344-351.
38 J. Lesage de la Haye, X. Zhang, I. Chaduc, F. Brunel, M. Lansalot and F. D'Agosto, *Angew. Chem. Int. Ed.*, 2016, **55**, 3739-3743.
39 Y. Zhang, M. Cao, G. Han, T. Guo, T. Ying and W. Zhang, *Macromolecules*, 2018, **51**, 5440-5449.
40 I. Gitsov and J. M. J. Frechet, *Macromolecules*, 1993, **26**, 6536-6546.
41 F. Wurm and H. Frey, *Prog. Polym. Sci.*, 2011, **36**, 1-52.
42 X. Liu and I. Gitsov, *Macromolecules*, 2019, **52**, 5563-5573.
43 J. del Barrio, L. Oriol, C. Sánchez, J. L. Serrano, A. Di Cicco, P. Keller and M.-H. Li, *J. Am. Chem. Soc.*, 2010, **132**, 3762-3769.
44 D. Huang, Y. Wang, F. Yang, H. Shen, Z. Weng and D. Wu, *Polym. Chem.*, 2017, **8**, 6675-6687.
45 Y. Zhou, W. Huang, J. Liu, X. Zhu and D. Yan, *Adv. Mater.*, 2010, **22**, 4567-4590.
46 C. Zhang, Y. Fan, Y. Zhang, C. Yu, H. Li, Y. Chen, I. W. Hamley and S. Jiang, *Macromolecules*, 2017, **50**, 1657-1665.
47 Y. Zheng, S. Li, Z. Weng and C. Gao, *Chem. Soc. Rev.*, 2015, **44**, 4091-4130.
48 R. Dong, Y. Zhou and X. Zhu, *Acc. Chem. Res.*, 2014, **47**, 2006-2016.
49 J. A. Alfurhood, H. Sun, P. R. Bachler and B. S. Sumerlin, *Polym. Chem.*, 2016, **7**, 2099-2104.
50 H. Han and N. V. Tsarevsky, *Chem. Sci.*, 2014, **5**, 4599-4609.
51 B. Yao, T. Hu, H. Zhang, J. Li, J. Z. Sun, A. Qin and B. Z. Tang, *Macromolecules*, 2015, **48**, 7782-7791.
52 E. Mohammadifar, A. Bodaghi, A. Dadkhahtehrani, A. Nemati Kharat, M. Adeli and R. Haag, *ACS Macro Lett.*, 2017, **6**, 35-40.
53 I. N. Kurniasih, J. Keilitz and R. Haag, *Chem. Soc. Rev.*, 2015, **44**, 4145-4164.
54 C. Liu, Y.-y. Fei, H.-l. Zhang, C.-y. Pan and C.-y. Hong, *Macromolecules*, 2019, **52**, 176-184.
55 M. Scharfenberg, J. Seiwert, M. Scherger, J. Preis, M. Susewind and H. Frey, *Macromolecules*, 2017, **50**, 6577-6585.
56 F. Li, M. Cao, Y. Feng, R. Liang, X. Fu and M. Zhong, *J. Am. Chem. Soc.*, 2019, **141**, 794-799.
57 Q. Wei, X. Zan, Q. Xianping, G. Öktem, K. Sahre, A. Kiriy and B. Voit, *Macromol. Chem. Phys.*, 2016, **217**, 1977-1984.
58 X.-X. Deng, F.-S. Du and Z.-C. Li, *ACS Macro Lett.*, 2014, **3**, 667-670.

59 X.-X. Deng, Y. Cui, F.-S. Du and Z.-C. Li, *Polym. Chem.*, 2014, **5**, 3316-3320.
60 Y. Shi, R. W. Graff, X. Cao, X. Wang and H. Gao, *Angew. Chem. Int. Ed.*, 2015, **54**, 7631-7635.
61 X. Cao, Y. Shi, X. Wang, R. W. Graff and H. Gao, *Macromolecules*, 2016, **49**, 760-766.
62 X. Cao, Y. Shi, W. Gan, H. Naguib, X. Wang, R. W. Graff and H. Gao, *Macromolecules*, 2016, **49**, 5342-5349.
63 Y. Shi, X. Cao, D. Hu and H. Gao, *Angew. Chem. Int. Ed.*, 2018, **57**, 516-520.
64 Y. Shi, X. Cao, S. Luo, X. Wang, R. W. Graff, D. Hu, R. Guo and H. Gao, *Macromolecules*, 2016, **49**, 4416-4422.
65 W. Gan, X. Cao, Y. Shi and H. Gao, *J. Polym. Sci., Part A: Polym. Chem.*, 2019, DOI: 10.1002/pola.29440.
66 D. Hölter, A. Burgath and H. Frey, *Acta Polym.*, 1997, **48**, 30-35.
67 E. R. Jones, M. Semsarilar, A. Blanazs and S. P. Armes, *Macromolecules*, 2012, **45**, 5091-5098.
68 L. A. Fielding, M. J. Derry, V. Ladmiral, J. Rosselgong, A. M. Rodrigues, L. P. D. Ratcliffe, S. Sugihara and S. P. Armes, *Chem. Sci.*, 2013, **4**, 2081-2087.
69 D. Li, M. Huo, L. Liu, M. Zeng, X. Chen, X. Wang and J. Yuan, *Macromol. Rapid Commun.*, 2019, **40**, 1900202.
70 E. R. Jones, M. Semsarilar, P. Wyman, M. Boerakker and S. P. Armes, *Polym. Chem.*, 2016, **7**, 851-859.
71 F. Brunel, J. Lesage de la Haye, M. Lansalot and F. D'Agosto, *J. Phys. Chem. B*, 2019, **123**, 6609-6617.
72 H. Hong, Y. Mai, Y. Zhou, D. Yan and J. Cui, *Macromol. Rapid Commun.*, 2007, **28**, 591-596.

This journal is © The Royal Society of Chemistry 20xx

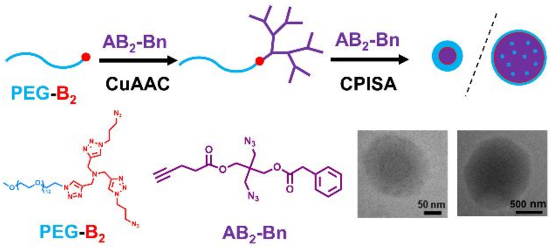

A one-pot method was developed for in situ preparation of linear-dendritic copolymer assemblies via click polymerization-induced self-assembly (CPISA).